Intra-operative near-infrared fluorescent cholangiography (NIRFC) in mouse models of bile duct injury

Jose-Luiz Figueiredo, MD, **Cory Siegel, MD**, **Matthias Nahrendorf, MD PhD**, and **Ralph Weissleder, MD PhD**

Center for Molecular Imaging Research, Massachusetts General Hospital and Harvard Medical School, Building 149, 13th St., Charlestown, MA 02129

Abstract

Background—Accidental injury to the common bile duct is a rare but serious complication of laparoscopic cholecystectomy. Accurate visualization of the biliary ducts may prevent or detect injuries early. Conventional X-Ray cholangiography is often used and can reduce the severity of injury when correctly interpreted. However, it may be useful to have an imaging method that could provide real-time extra-hepatic bile duct visualization without changing the field of view from the laparoscope. The purpose of this study was to use a new NIR fluorescent agent that is rapidly excreted via the biliary route in pre-clinical models to evaluate intra-operative real time near infrared fluorescent cholangiography (NIRFC).

Methods—To investigate probe function and excretion, a lipophilic near infrared fluorescent agent with hepatobiliary excretion was injected intravenously into one group of C57/BL6 control mice and four groups of C57/BL6 mice with the following experimentally-induced conditions: a) chronic biliary obstruction, b) acute biliary obstruction c) bile duct perforation and e) choledocholithiasis, respectively. The biliary system was imaged intravitally for one hour using near-infrared fluorescence (NIRF) with an intra-operative small animal imaging system (excitation 649 nm, emission 675 nm).

Results—The extra hepatic ducts and extra-luminal bile were clearly visible due to the robust fluorescence of the excreted fluorochrome. Twenty-five minutes after intravenous injection, the target-to-background ratio peaked at 6.40 ± 0.83 but was clearly visible for ~ sixty minutes. The agent facilitated rapid identification of biliary obstruction and bile duct perforation. Implanted beads simulating choledocholithiasis were promptly identifiable within the common bile duct lumen.

Conclusions—NIRF agents with hepatobiliary excretion may be used intra-operatively to visualize extra hepatic biliary anatomy and physiology. Used in conjunction with laparoscopic imaging technologies this should enhance hepatobiliary surgery.

Keywords

cholangiography; fluorescence; laparoscopic cholecystectomy; complications; surgical injuries; bile duct injuries

Corresponding author: Ralph Weissleder, MD PhD, MGH-CSB, CPZN-5206, 185 Cambridge Street, Boston, MA 02114, Tel: 617-726-8226, Fax: 617-726-5708, rweissleder@mgh.harvard.edu.

Introduction

Laparoscopic cholecystectomy (LC) is one of the most frequently performed surgical procedures and typically has a relatively low complication rate (0.15%) [1,2]. However, accidental bile duct injuries are of concern as they can have dire consequences for the patient when they occur [3]. Mild injuries, including cystic duct leakage and bile duct strictures are usually treated endoscopically and/or interventionally, while major injuries with leakage or complete transection of common bile duct (CBD) often require open surgery such as hepatico-jejunostomy [4,5].

Video laparoscopic cholecystectomy uses high definition cameras to give a panoramic intra-abdominal field of view. However, even with this technology, inflammation, adhesions or surrounding fat sometimes impede visualization of the biliary ducts [6]. Studies suggest that a majority of iatrogenic biliary injuries are secondary to misidentification of the biliary anatomy and that 60–90% of injuries are only identified post-operatively [7–10]. If the biliary system is perforated, repair is difficult, requires specialized centers and can occasionally cause life-threatening situations [11]. In addition, these injuries and their repairs can have profound long-term consequences. There have been reports of up to 4% postoperative mortality and greater than 40% complication rate from biliary repair of bile duct injuries sustained during laparoscopic cholecystectomy with a high rate of long-term sequelae including infections, cholangitis, and anastomosis leaks [12,13].

X-ray intra-operative cholangiography (IOCG) has long been used for hepatobiliary surgeries [14] and is considered a safe procedure. However, there has been discussions regarding routine IOCG in laparoscopic cholecystectomy with regard to procedure logistics, intralaparoscopic catheterization of the gall bladder or the cystic duct, time considerations and immediate interpretation [15,16]. Depending on the needs of the surgeon and available resources, in some cases it may be prudent to have a less invasive technique that allows for straightforward intra-operative identification of the extra-biliary structures. Such methods could facilitate isolation of the cystic duct, identify common biliary duct strictures, prevent complications and could potentially be used as an alternative or complementary addition to X-ray cholangiography.

Fluorescent intra-operative cholangiography has been tested both experimentally [17,18] and clinically (19–21) to evaluate its use as a preventive and diagnostic technique. While these studies introduced the necessary optical instrumentation, an improvement in fluorescent signal-to-noise ratio (SNR) and decrease of background signal would further enhance this real-time procedure and directly impact the target identification. Imaging in the far red and near-infrared spectrum would satisfy these requirements since light in this range can penetrate tissues as deep as the thickness of the human bile duct wall (22,23). Thus, this method could facilitate intra-operative visualization of the extra-hepatic biliary anatomy prior to dissection. The choice of specific wavelength is primarily governed by quantum yield, auto-fluorescence and SNR considerations of a given fluorochome. The majority of agents have been developed for the 650–800 nm excitation range.

We have previously reported on the use of a NIR calcium-binding fluorescent probe for intra-operative detection of nephrolithiasis [24]. In this study, the renal excretion of a fluorescent probe was critical in visualizing small intra-pelvic stones. In analogy, the development of intravenously administered near infrared fluorescent (NIRF) agents with hepatobiliary rather than renal excretion could aid laparoscopic hepatobiliary surgery. The purpose of this study was to use a new NIR fluorescent agent that is rapidly excreted via the biliary route in pre-clinical models to evaluate intra-operative real-time near infrared fluorescent cholangiography (NIRFC).

Materials and Methods

Animal models

All experiments were approved by the Institutional Review Board and performed in adult C57/ BL6 female mice (25–30g, n=16), obtained from Charles River Laboratories, Inc. (Wilmington, MA). Animals were physiologically monitored with pulse oximetry and body temperature during and after all procedures. Mice were anesthetized with a mixture of ketamine (90 mg/kg) and xylazine (10mg/kg), which were injected intraperitoneally. In order to best simulate true intra-operative conditions, a transversal laparotomy was performed to fully expose the peritoneal cavity for *in vivo* imaging of the biliary system.

To investigate the fluorescent signal inside the biliary ducts over time, target-to-background ratios (TBR) were determined in five groups of mice: four surgically-induced models of a) chronic biliary obstruction b) acute biliary obstruction, c) acute biliary perforation, and d) choledocholithiasis model; and one control group.

Control (N=4)

Mice underwent laparotomy without manipulation of the biliary system. Each mouse was then injected intravenously with 10 nmol of fluorescent agent and the biliary system was imaged at 5-minute intervals for one hour. One mouse was additionally imaged at 1 minute and 3 minutes post-injection to explore probe signal in the vasculature.

Chronic biliary obstruction model (N=3)

The common bile duct was partially occluded using a 10-0 Prolene suture and then both the peritoneal cavity and skin were closed with Ethicon Prolene 6-0 sutures (Johnson & Johnson, Brussels, Belgium). The animals were allowed to recover for two weeks after which they underwent a second laparotomy for imaging.

Acute biliary obstruction model (N=3)

The common bile duct was completely occluded using 10-0 Ethicon Prolene suture (Johnson & Johnson, Brussels, Belgium). The fluorescent contrast agent was injected one minute after injury to imitate an intra-operative scenario of suspected accidental duct ligation. The mice were then imaged at 5-minute intervals for a period of 30 minutes, while the duct was obstructed. The occluding suture was subsequently released and mice were imaged again to investigate the resumption of biliary drainage through the common bile duct and into the duodenum.

Acute biliary perforation model (N=3)

After laparotomy, 10 nmol of the fluorescent probe was injected. Imaging began 5 minutes after injection to establish that the imaging agent was within the biliary system. After 5 minutes, the mouse was removed from the imaging platform and under microscope guidance the common bile duct was perforated just distal to its origin, using micro-surgical scissors. The mouse was immediately placed back into the imaging apparatus for 30 minutes to visualize the leak of bile from the damaged common bile duct. The perforation was carried out following probe injection for both anatomical comparison and for simulation of a routine pre-surgical probe injection (done to aid perforation detection).

Choledocholithiasis model (N=3)

The abdominal cavity was opened and a small incision was made in the gallbladder fundus. Two white zirconia silica beads with 100 µm diameter (Biospec Products, Bartlesville, OK) were placed through the incision into the gallbladder fundus. The incision was closed using

Prolene 10-0 and the beads were observed whilst they traveled into the common bile duct. The animal was then injected with 10 nmol of the NIR probe and imaged. Subsequent white light images were acquired with a digital camera. White beads were selected so that they could be easily located under white light imaging and compared to the near-infrared channel.

Imaging agent

We used VM674 (VisEn Medical, Bedford, MA), a near-infrared lipophilic fluorochrome probe exhibiting rapid biliary excretion following intravenous administration. The fluorophore is a small molecule in the indocyanine class with a molecular weight of ~900g/mol and an absorption maximum of 675 nm in MeOH. In aqueous media, the excitation maximum is at 672 nm and the emission maximum is at 692 nm. The extinction coefficient is 180,000/M/cm (mono TEA salt in MeOH). Prior to use, the agent was diluted in 100 µL of phosphate buffered saline (PBS). The probe was injected intravenously via tail vein at a dose of 10 nmol/mouse.

Imaging and data analysis

All fluorescent imaging studies were performed using an OV-110™ Small Animal Imaging System (Olympus, Center Valley, PA), a hybrid of a planar reflectance fluorescence imaging system and a high-power microscope. The mice were imaged using bright field and near-infrared fluorescence (excitation 649 nm, emission 675 nm) with up to 8-times magnification. Animals were placed on a temperature-controlled platform and intra-operative images of liver, gall bladder, bile ducts and duodenum were serially acquired. Image acquisition time was 100ms per frame. White light images were acquired with a handheld digital camera (Olympus FE-280, Center Valley, PA).

Images were analyzed using circular regions of interest of 0.3 mm diameter. Mean signal intensity and its standard deviation was quantified using Osirix software (Geneva, Switzerland) on a Macintosh computer. Merging of white light and fluorescent images was accomplished with a best-fit fusion implemented on Osirix software. The target-to-background ratio (TBR) was calculated as follows: TBR = (Target - Noise)/(Background - Noise), where the background is normal adjacent liver tissue and the target is the region of interest, i.e. the common bile duct. Noise was recorded in a region outside the mouse. All statistical analyses were performed using Prism software (Graphpad Software, San Diego, CA). Mean values were compared using unpaired Student's t-test and with ANOVA correction for multiple comparisons. $P < 0.05$ was considered statistically significant. Data is given in as mean $+/-$ SD.

Results

Following intravenous administration of VM674, the biliary system became readily visible (Fig 1 and 2). Negligible background fluorescent signal was observed in the near infrared prior to probe injection (Fig 1A). During intravenous administration and up to one-minute post injection, a very low fluorescent signal was detected in the hepatic vasculature (Fig 1B). Between 2–5 minutes, the biliary signal increased, allowing delineation of the extra-hepatic biliary anatomy (Fig 1C). Fluorescent signal peaked at 25 minutes post-injection (TBR 6.40 ± 0.83) and remained elevated for 60 minutes (Fig 2).

In the chronic biliary obstruction model, inflammation, fibrosis and fat tissue made it difficult to localize the site of the obstruction with white light (Fig 3A). In contradistinction, the NIR fluorescent agent readily identified the stenotic area and proximal dilation (Fig 3B, C). The TBR in the region proximal to the obstruction was significantly higher than in the distal duct (8.53± 0.63 versus 4.96 ± 1.29, respectively) p=0.0340.

In the acute obstruction model, the ligature of the bile duct and proximal dilation (Fig 4A) was easily identified in NIR imaging (Fig 4B). High fluorescent signal intensity was noted in the common bile duct proximal to the obstruction site and no signal was obtained distal to the ligation. Once the biliary duct ligature was released and bile flow resumed, minimal difference was observed in bright field view (Fig 4C); although the fluorescent probe easily delineated the bile duct anatomy distal to the ligature (Fig 4D). Quantification of NIR signal showed a significantly increased TBR proximal to the obstruction (7.33 ± 0.78) and distal to the obstruction site (6.73 ± 1.26) once bile flow was allowed to resume, when compared to the unenhanced bile duct (0.36 ± 0.07) p=0.0036 and p=0.0004 respectively.

To reproduce a model of biliary trauma with bile leakage, fluorescent images of the bile duct were obtained prior to the bile duct injury but five minutes after probe injection (Fig 5A). Following intentional bile duct perforation, intra-abdominal free bile was not easily identified with the naked eye (Fig 5B). However, the localization of the perforation site was greatly enhanced using NIR imaging, which also localized bile extravasations into the abdominal cavity (Fig 5C, D). Statistical analyses revealed a significantly higher TBR (5.43 ± 0.66) for the extravasated bile when compared to the same anatomical region prior to CBD perforation (0.81 ± 0.08) p=0.0011

To model choledocholithiasis, synthetic micro beads (100 µm diameter) were implanted into the common bile duct (Fig 6A, B). After probe injection, the absolute fluorescent signal intensity was 2.9 times greater in the lumen of the duct as compared to a region of interest placed over the area of the implanted beads. Thus, NIR imaging allowed prompt intra-operative identification of beads (Fig 6C, D). The difference in signal intensity provided significant negative contrast when comparing the TBRs (5.89 ± 1.09 for bile, 2.40 ± 0.42 for the beads) p=0.0200.

Discussion

NIRFC imaging of a biliary excreted NIR probe facilitates intra-operative visualization of the bile ducts in real-time and high definition and allows for rapid identification of bile duct anatomy and pathology. Clinically, identification of free bile in the abdominal cavity confirms bile duct transection or perforation. However, during conventional laparoscopic cholecystectomy it is difficult to distinguish a small amount of extra-luminal bile from a mixture of blood and transudations in the surgical field [25,26]. Moreover, unintentional small bile duct ligature may occur and is usually not detected immediately. These two situations are responsible for the majority of intra-operative bile duct injuries [27].

X-ray cholangiography is a standard clinical imaging technique used during cholecystectomy surgeries, the benefits of which have been well researched and demonstrated [28]. Its routine intra-laparoscopic use is still debated by some and the decision to perform IOCG depends on each surgeon's experience and local facilities [29–31]. Most commonly, intra-laparoscopic cholangiography is used when bile duct injuries are suspected.

In the clinical setting, a video laparoscopic imaging system could potentially provide multiple channels integrating white light and fluorescent light sources and several such systems have already been described [32–34]. Images could be fused in real-time and thus provide the surgeon with additional information regarding anatomy and bile leaks. Theoretically, fluorescent intra-operative cholangiography could be done easily by injecting the fluorescent contrast agent and switching the camera from color to infrared lighting. However, intra-operative fluorescent imaging using shorter wavelength light [17,18] has shown lower achievable TBRs due to absorbance of endogenous fluorochromes such as hemoglobin, melanin, and water.

Imaging hepatic excretion of indocyanine green (ICG) could be used as an alternative method to increase fluorescence [19–21]. However, because ICG highlights both vasculature and biliary anatomy, it could result in difficulties distinguishing them intra-laparoscopically. Moreover, ICG is also dependent on cardiac and hepatic function. Thus, the use of the presented lipophilic indocyanine-based NIR fluorescent agent designed for hepatobiliary excretion imaging without fluorescence during the vascular time allows for clear differentiation of vessels from bile ducts.

The fluorescent agent used in the current experiment has absorption/emission peaks at 675/692 nm, but more importantly, it has ideal pharmacokinetic properties, which enhance extra-hepatic bile duct imaging with little background from the portal hepatis. An additional problem, common with fluorescent imaging, is the low penetration depth of light through tissue matter. However, considering that the thickness of a normal human bile duct wall and wall thickness in a biliary obstruction situation is 0.6 ± 0.3 mm and 0.8 ± 0.5 mm, respectively [26], the low penetration depth would be unlikely to pose a problem and our strategy would therefore be suitable for laparoscopic cholecystectomy [35]. The penetration of NIR light is dependent on tissue absorption, scatterings, auto fluorescence and wavelengths/illumination [36]. The higher the wavelength, the better the signal-to-noise ratio. In a reflectance mode such as the one used here, maximum penetration depths are usually ~ 5–8 mm, before scattering degrades image quality [37]. In tomographic mode however, penetration depths increase considerably to several centimeters [38]. It is thus not inconceivable to devise hand held tomographic scanner units similar to intra-operative ultra-sounds probes [39].

In high definition and real-time, we observed the NIR probe moving from the hepatic parenchyma towards the biliary ducts, as early as three minutes after intravenous administration. From 5 to 60 minutes post-injection, a bright fluorescent signal was seen inside the biliary ducts with low hepatic background signal. Intra-operative imaging facilitated identification of the dilation/stricture area in a bile duct stenosis model. Similarly, perforation of the common bile duct was easily located at the site where the bile and the probe leaked into the abdominal cavity. Synthetic beads were used to model bile stones and were readily identified within the lumen of the common bile duct, suggesting easy intra-operative identification and localization of choledocholithiasis.

Since the probe reaches the biliary system within minutes, a patient could be injected with the agent following anesthesia induction or during placement of the laparoscopic instruments. This would allow the probe to reach far within the extra-hepatic biliary system at the beginning of the surgery exploration. NIRFC could be used as a routine procedure, as has been suggested for intra-operative X-ray cholangiography. NIRFC could also be possibly used in patients falling into high-risk categories for development of complications or in those undergoing a second operation to repair suspected iatrogenic injuries. Alternatively, since the signal is bright at five minutes post-injection, the probe could be injected intra-operatively at any point or re-injected multiple times to assess for suspected biliary injury. In addition, post-operative patients necessitating drain placement could be injected with the fluorescent agent and have drain contents examined at the bedside with a portable NIR source.

Conclusion

We have used a biliary-excreted near-infrared fluorescent probe for rapid and sustained visualization of biliary anatomy with a desirable target-to-background ratio. In several mouse models of biliary injury, we have investigated how intra-operative NIRFC imaging could prevent complications and rapidly identify biliary injury. Although this was an observational study using mouse subjects, we believe that given the aforementioned inherent properties of NIRF imaging, such an agent may be feasible and desirable to use in humans. Further studies

would be necessary to elucidate the potential use of NIRFC in humans within a practical clinical setting, i.e. to determine how room lighting would be optimized, how and when the agent would be administered and the effective penetrance of fluorescence. NIRFC imaging technology could be developed for and integrated into existing video laparoscopic systems and would be clinically helpful to prevent or diagnose intra-operative bile duct injury.

Acknowledgments

References

1. Dolan JP, Diggs BS, Sheppard BC, Hunter JG. Ten-year trend in the national volume of bile duct injuries requiring operative repair. Surg Endosc 2005;19(7):967–973. [PubMed: 15920680]

2. Dolan JP, Diggs BS, Sheppard BC, Hunter JG. The National Mortality Burden and Significant Factors Associated with Open and Laparoscopic Cholecystectomy: 1997–2006. J Gastrointest Surg. 2009 Sep 2; (Epub ahead of print).

3. Saad N, Darcy M. Iatrogenic bile duct injury during laparoscopic cholecystectomy. Tech Vasc Interv Radiol 2008;11:102–110. [PubMed: 18922455]

4. Karvonen J, Gullichsen R, Laine S, Salminen P, Gronroos JM. Bile duct injuries during laparoscopic cholecystectomy: Primary and long-term results from a single institution. Surg Endosc 2007;21:1069–1073. [PubMed: 17514397]

5. Abdel Wahab M, el-Ebiedy G, Sultan A, el-Ghawalby N, Fathy O, Gad el-Hak N, Abo Elenin A, Abo Zid M, Ezzat F. Postcholecystectomy bile duct injuries: Experience with 49 cases managed by different therapeutic modalities. Hepatogastroenterology 1996;43:1141–1147. [PubMed: 8908542]

6. Georgiades CP, Mavromatis TN, Kourlaba GC, Kapiris SA, Bairamides EG, Spyrou AM, Kokkinos CN, Spyratou CS, Ieronymou MI, Diamantopoulos GI. Is inflammation a significant predictor of bile duct injury during laparoscopic cholecystectomy? Surg Endosc 2008;22:1959–1964. [PubMed: 18443865]

7. Francoeur JR, Wiseman K, Buczkowski AK, Chung SW, Scudamore CH. Surgeons' anonymous response after bile duct injury during cholecystectomy. Am J Surg 2003;185:468–475. [PubMed: 12727569]

8. Hugh TB. New strategies to prevent laparoscopic bile duct injury--surgeons can learn from pilots. Surgery 2002;132:826–835. [PubMed: 12464867]

9. Olsen D. Bile duct injuries during laparoscopic cholecystectomy. Surg Endosc 1997;11:133–138. [PubMed: 9069144]

10. Slater K, Strong RW, Wall DR, Lynch SV. Iatrogenic bile duct injury: The scourge of laparoscopic cholecystectomy. ANZ J Surg 2002;72:83–88. [PubMed: 12074081]

11. Gevers JK. [claims for damages due to bile-duct injury following laparoscopic cholecystectomy: Some legal remarks]. Ned Tijdschr Geneeskd 2007;151:1713–1715. [PubMed: 17784692]

12. Sicklick JK, Camp MS, Lillemoe KD, Melton GB, Yeo CJ, Campbell KA, Talamini MA, Pitt HA, Coleman J, Sauter PA, Cameron JL. Surgical management of bile duct injuries sustained during laparoscopic cholecystectomy: Perioperative results in 200 patients. Ann Surg 2005;241:786–792. discussion 793-5. [PubMed: 15849514]

13. Walsh RM, Henderson JM, Vogt DP, Brown N. Long-term outcome of biliary reconstruction for bile duct injuries from laparoscopic cholecystectomies. Surgery 2007;142:450–456. discussion 456-7. [PubMed: 17950335]

14. Mirizzi PL. Operative cholangiography. Surg Gynaecol Obstet 1937;65:702–710.

15. Livingston EH, Mller JA, Coan B, Rege RV. Cost and utilization of intraoperative cholangiography. J Gastrointest Surg 2007;11(9):1162–1167. [PubMed: 17602271]

16. Ciulla A, Agnello G, Tomasello G, Castronovo G, Maiorana AM, Genova G. the intraoperative cholangiography during videolaparoscopic cholecystectomy. What is its role? Results of a non-randomized study. Ann Ital Chir 2007;78:85–89. [PubMed: 17583116]

17. Stiles BM, Adusumilli PS, Bhargava A, Fong Y. Fluorescent cholangiography in a mouse model: An innovative method for improved laparoscopic identification of the biliary anatomy. Surg Endosc 2006;20:1291–1295. [PubMed: 16858526]

18. Holzinger F, Krahenbuhl L, Schteingart CD, Ton-Nu HT, Hofmann AF. Use of a fluorescent bile acid to enhance visualization of the biliary tract and bile leaks during laparoscopic surgery in rabbits. Surg Endosc 2001;15:209–212. [PubMed: 11285970]

19. Araki K, Namikawa K, Mizutani J, Doiguchi M, Yamamoto H, Arai H, Yamaguchi T, Ido Y, Uno K, Hayashi N. Indocyanine green staining for visualization of the biliary system during laparoscopic cholecystectomy. Endoscopy 1992;24:803. [PubMed: 1468406]

20. Aoki T, Murakami M, Yasuda D, Kusano T, Matsuda K, Niiya T, Kato H, Murai N, Otsuka K, Kusano M, Kato T. Intraoperative fluorescent imaging using indocyanine green for liver mapping and cholangiography. J Hepatobiliary Pancreat Surg. 2009 (Epub ahead of print).

21. Tagaya N, Shimoda M, Kato M, Nakagawa A, Abe A, Iwasaki Y, Oishi H, Shirotani N, Kubota K. Intraoperative exploration of biliary anatomy using fluorescence imaging of indocyanine green in experimental and clinical cholecystectomies. 2009 (Epub ahead of print).

22. Tamada K, Tomiyama T, Oohashi A, Aizawa T, Nishizono T, Wada S, Tano S, Miyata T, Satoh Y, Ido K, Kimura K. Bile duct wall thickness measured by intraductal US in patients who have not undergone previous biliary drainage. Gastrointestinal endoscopy 1999;49(2):199–203. [PubMed: 9925698]

23. Faris F, Thornliey M, Wickramasinghe Y, Houston R, Rolfe P, Livera N, Spencer A. Non-invasive in vivo near-infrared optical measurement of the penetration depth in the neonatal head. Phys Physiol Meas 1991;12(4):353–358.

24. Figueiredo JL, Passerotti CC, Sponholtz T, Nguyen HT, Weissleder R. A novel method of imaging calcium urolithiasis using fluorescence. J Urol 2008;179:1610–1614. [PubMed: 18295253]

25. Sammak BM, Yousef BA, Gali MH, al Karawi MA, Mohamed AE. Case report: Radiological and endoscopic management of bile leak following laparoscopic cholecystectomy. J Gastroenterol Hepatol 1997;12:34–38. [PubMed: 9076620]

26. Peters JH, Ollila D, Nichols KE, Gibbons GD, Davanzo MA, Miller J, Front ME, Innes JT, Ellison EC. Diagnosis and management of bile leaks following laparoscopic cholecystectomy. Surg Laparosc Endosc 1994;4:163–170. [PubMed: 8044356]

27. Suhocki PV, Meyers WC. Injury to aberrant bile ducts during cholecystectomy: A common cause of diagnostic error and treatment delay. AJR Am J Roentgenol 1999;172:955–959. [PubMed: 10587128]

28. Sarli L, Costi R, Roncoroni L. Intraoperative cholangiography and bile duct injury. Surg Endosc 2006;20:176–177. [PubMed: 16333543]

29. Pisano G, Licheri S, Dazzi C, Erdas E, Pomata M, Daniele GM. Operative cholangiography during laparoscopic cholecystectomy: Considerations about routine or selective policy. G Chir 2005;26:333–337. [PubMed: 16329778]

30. Wenner DE, Whitwam P, Turner D, Kennedy K, Hashmi S. Actual time required for dynamic fluoroscopic intraoperative cholangiography. Jsls 2005;9:174–177. [PubMed: 15984705]

31. Karthikesalingam A, Markar SR, Weerakkody R, Walsh SR, Carroll N, Praseedom RK. Radiation exposure during laparoscopic cholecystectomy with routine intraoperative cholangiography. Surg Endosc. 2009 Jan 1; [Epub ahead of print].

32. Tanaka E, Choi HS, Humblet V, Ohnishi S, Laurence RG, Frangioni JV. Real-Time Intra-operative Assessment of the Extra hepatic Bile Ducts in Rats and Pigs Using Invisible Near-Infrared Fluorescent Light. Surgery 2008;144(1):39–48. [PubMed: 18571583]

33. Kawashima T, Naraoka S, Kakizaki T. Intraoperative graft assessment using fluorescent imaging system (SPY). Kyobu Geka 2009;62(7):519–522. [PubMed: 19588820]

34. Aoki T, Yasuda D, Shimizu Y, Odaira M, Niiya T, Kusano T, Mitamura K, Hayashi K, Murai N, Koizumi T, Kato H, Enami T, Miwa M, Kusano M. Image-Guided liver Mapping Using Fluorescence Navigation System with Indocyanine Green for Anamical Hepatic Resection. World Journal of Surgery 2008;32(8):1763–1767. [PubMed: 18543027]

35. Fantini S, Hueber D, Franceschini MA, Gratton E, Rosenfeld W, Stubblefield PG, Maulik D, Stankovic MR. Non-invasive optical monitoring of the newborn piglet brain using continuous-wave and frequency-domain spectroscopy. Phys. Med. Biol 1999;44:1543–1563. [PubMed: 10498522]

36. Lin B, Chernomordik V, Gandjbakhche A, Matthews D, Demos S. Investigation of signal dependence on tissue thickness in near infrared spectral imaging. Optical Express 2007;15(25):16581–16595.

37. Franceschini MA, Gratton E, Hueber D, Fantini S. near-infrared absorption and scattering spectra of tissues in vivo. Proceedings of SPIE 1999;3597:526–531.

38. Heintz A, Hohne U, Schweden F, Junginger T. Preoperative detection of intrathoracic tumor spread of esophageal cancer: endosonography versus computed tomography. Surgical Endoscopy 1991;5 (2):75–78. [PubMed: 1948618]

39. Ge J, Zhu B, Regalado S, Godavarty A. Three-dimensional fluorescence – enhanced optical tomography using a hand-held probe based imaging system. Med. Phys 2008;35(7):3354–3363. [PubMed: 18697559]
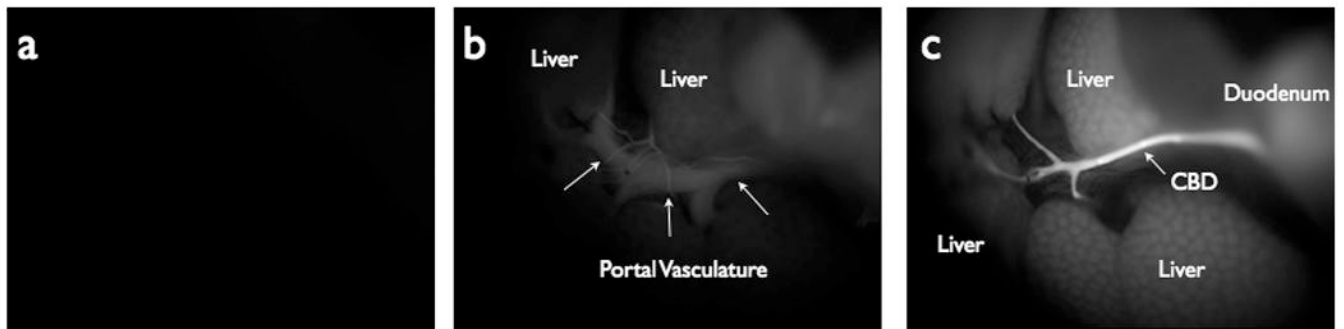
Figure 1.
Near Infrared Fluorescent (NIRF) images demonstrating probe accumulation in the biliary system. (A) NIRF image taken prior to probe injection. (B) NIRF image taken at T=1 minutes post-injection, showing probe within hepatic vasculature and initial accumulation in the liver. (C) NIRF image at T=3 minutes post-probe injection, showing high fluorescent signal in the biliary tree and comparatively low signal in the vasculature.
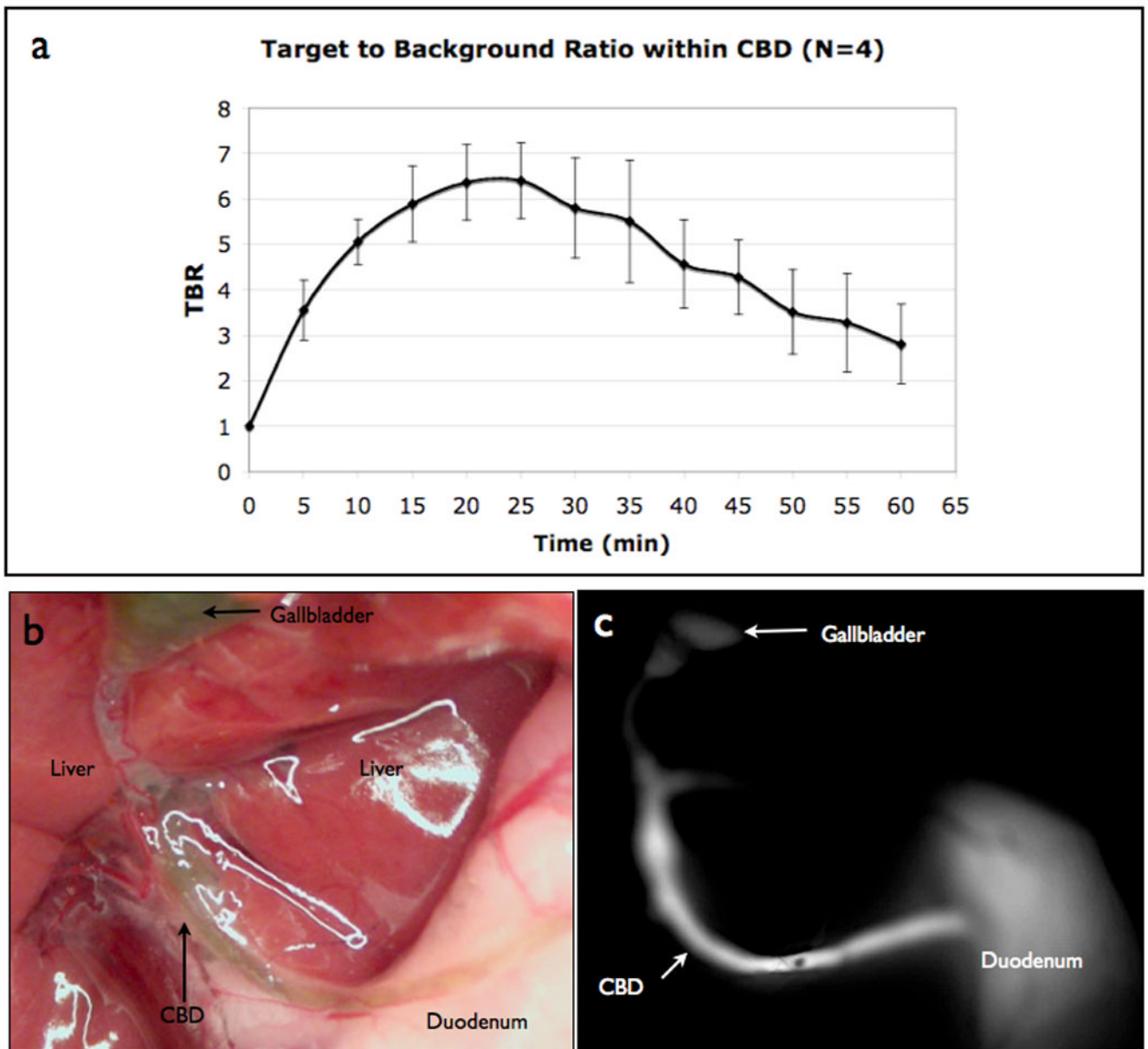
Figure 2.
Near Infrared Fluorescent Cholangiography (NIRFC) of normal bile duct anatomy. (A) TBR of the NIRF probe in the common bile duct over time from control mice (N=4). (B) Color picture showing gall bladder, common bile duct and duodenum anatomy. (C) NIRFC imaging of gall bladder, common bile duct and duodenum at peak TBR, 25 minutes after probe injection.
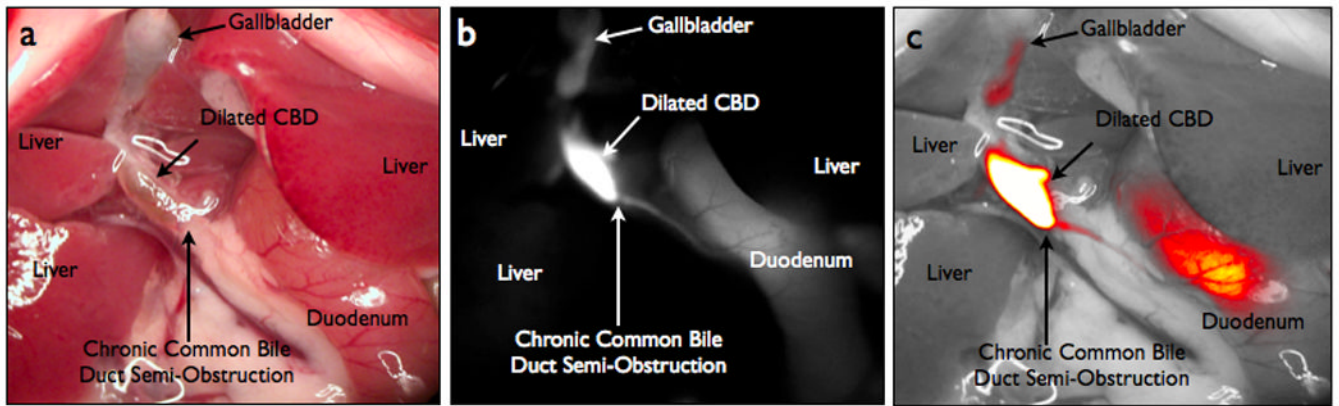
Figure 3.
NIRFC of a chronic biliary obstruction model. (A) Color image of a chronic biliary obstruction model. (B) Biliary chronic obstruction in NIRFC view. (C) Merged white light and NIRFC image.
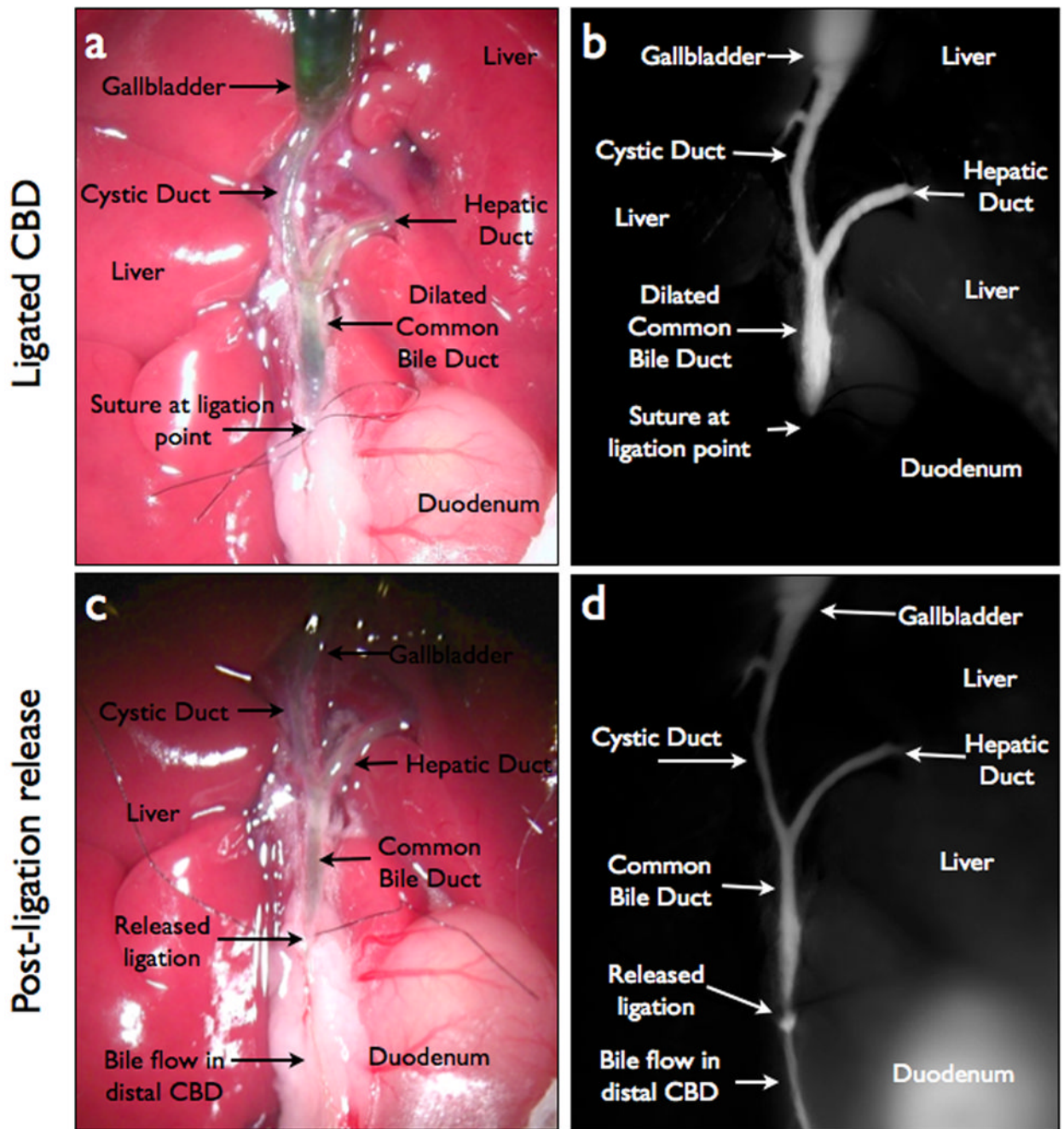
Figure 4.
NIRFC of an acute biliary obstruction model. (A) Color image of acute obstruction model, showing dilated ducts and ligation point. (B) NIRFC image of acute obstruction model with VM674. (C) Color image of acute obstruction model after the suture at ligation point is released. (D) NIRFC image with VM674 after ligation is released in acute obstruction, showing resumption of bile flow through common bile duct into duodenum.
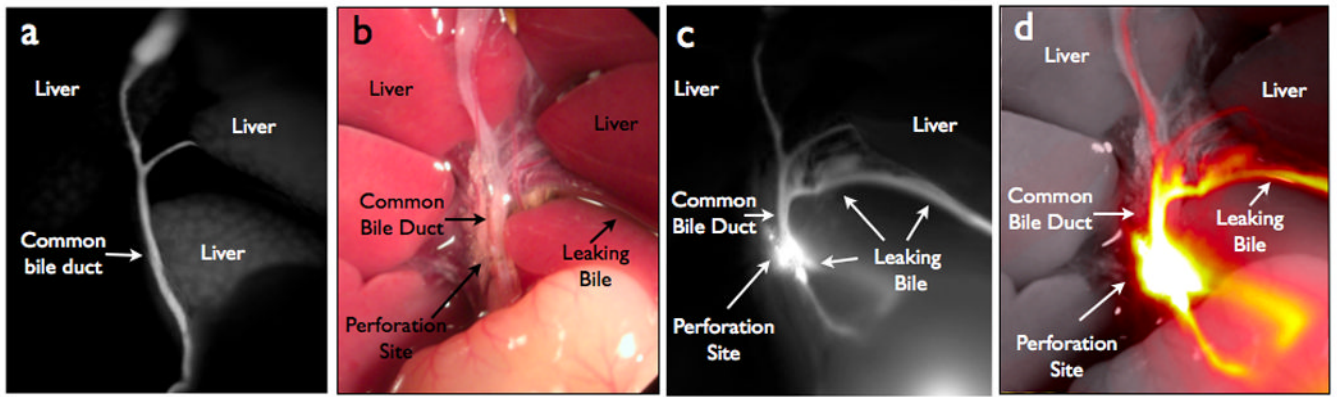
Figure 5.
NIRFC of bile duct leak model. (A) NIRFC image of biliary anatomy prior to perforation of common bile duct. (B) Color image of bile leak model after perforation. (C) NIRFC image of biliary anatomy with perforation site and extravasated bile. (D) Merged white light and NIRFC image.
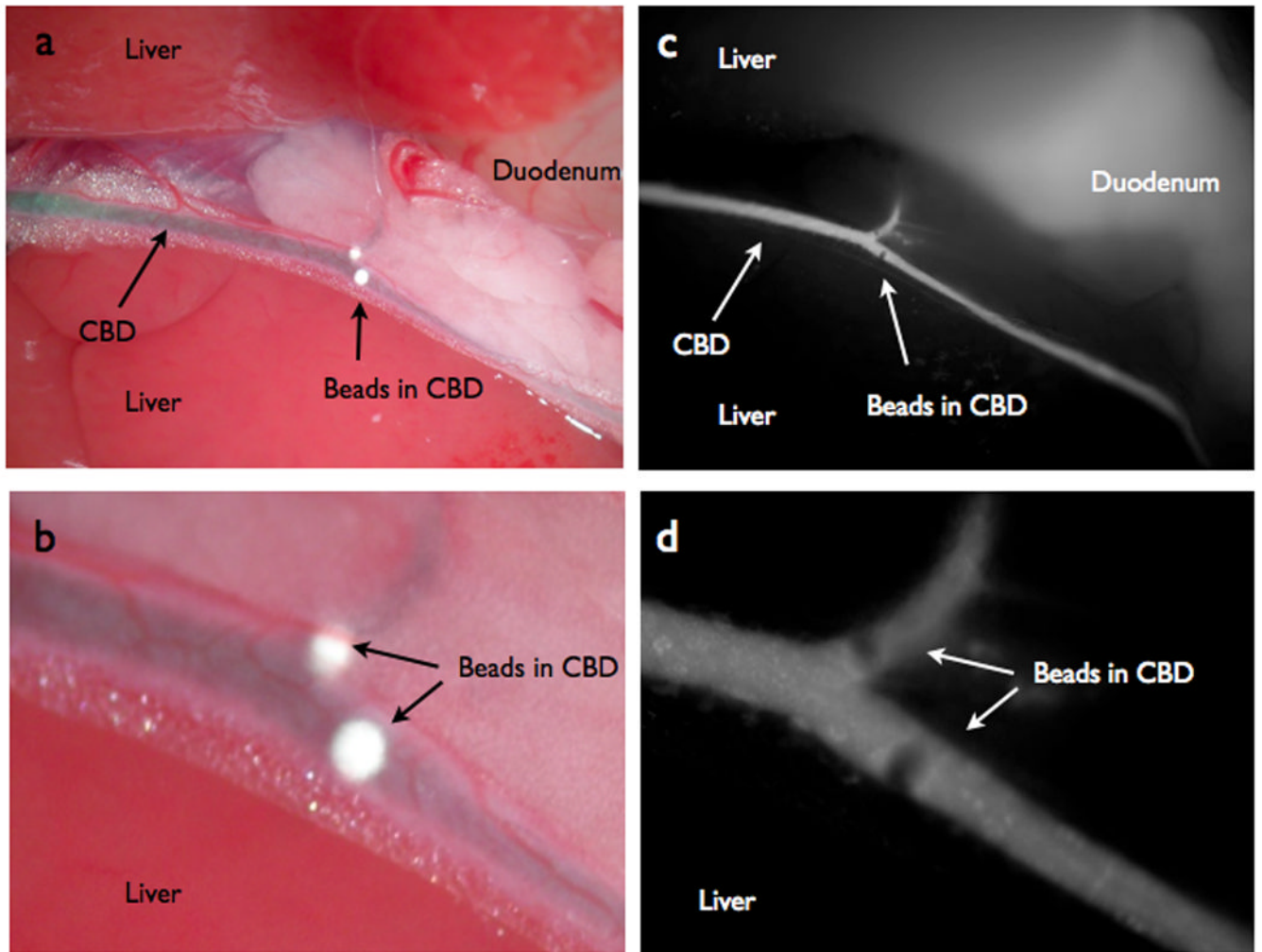
Figure 6.
NIRFC of choledocholithiasis model. (A) Color image depicting white 100µm diameter beads inside the lumen of the common bile duct simulating choledocholithiasis. (B) Color zoom image of the beads. (C) NIRFC imaging of the same beads in lumen of CBD. (D) NIRFC zoom image of beads.